Nationaal Lucht- en Ruimtevaartlaboratorium
National Aerospace Laboratory NLR

NLR-TP-98264

Failure criterion for the skin-stiffener interface in composite aircraft panels

J.C.F.N. van Rijn

Nationaal Lucht- en Ruimtevaartlaboratorium

National Aerospace Laboratory NLR

NLR-TP-98264

Failure criterion for the skin-stiffener interface in composite aircraft panels

J.C.F.N. van Rijn

This investigation has been carried out under a contract awarded by the Netherlands Agency for Aerospace Programmes, contract number 01310N.
The Netherlands Agency for Aerospace Programmes has granted NLR permission to publish this report.

This report is based on an article to be published in the proceedings of the Thirteenth Technical Conference of the American Society for Composites.

Division:	Structures and Materials
Issued:	10 June 1998
Classification of title:	Unclassified

Contents

This page is intentionally left blank.

FAILURE CRITERION FOR THE SKIN-STIFFENER INTERFACE IN COMPOSITE AIRCRAFT PANELS

J.C.F.N. van Rijn
National Aerospace Laboratory NLR
Amsterdam, The Netherlands

ABSTRACT

In numerous panel tests it was established that, in the post-buckling regime, failure of a composite stiffened panel is often induced by failure of a skin-stiffener interface. The present paper describes recent and on-going research performed at the National Aerospace Laboratory NLR, which aims at the derivation of a failure criterion for stiffener pop-off.
The strip specimens used in the present investigation consisted of a tapered stiffener flange bonded on a skin laminate. The specimens were loaded in four-point bending.
It was established that there was no significant influence of the stiffness properties of the flange laminate on the skin-stiffener interface strength. The strength of the skin-stiffener interface was governed by the deformation of the skin only.

INTRODUCTION

In numerous panel tests it was established that, in the post-buckling regime, failure of a composite stiffened panel is often induced by failure of a skin-stiffener interface. It was therefore deemed necessary to include a failure criterion for the skin-stiffener interface as a constraint in the panel design optimization code PANOPT. PANOPT was developed at the National Aerospace Laboratory NLR for the design of stiffened composite panels for primary aircraft structures with buckling and post-buckling constraints (Ref. 1).

Earlier research at the NLR, aimed at the development of a failure criterion for the skin-stiffener interface, was reported in references 2 and 3.
In reference 2 the results of an experimental programme on strip specimens with a secondarily bonded blade-type stiffener was presented. The specimens were tested in four point bending, under lateral tension of the skin, and with a pull-off test. An evaluation of the results was performed, using an analytical solution for the stress distribution in a lap joint configuration.
In reference 3 the results of an experimental programme on similar strip specimens is given. Here, the influence of various manufacturing techniques and stiffener flange details on the strength of the skin-stiffener interface was established. The specimens were tested under lateral tension of the skin and with a pull-off test.

Research using a similar type of specimen is reported in references 4 and 5. However, the specimens used were further simplified by eliminating the stiffener web.
In reference 4 the influence of the taper on the flange was investigated under three-point and four-point bending configurations. The results were evaluated using finite element analyses.
In reference 5 four different skin laminates and two flange laminates were used to establish the

influence of skin and flange lay-up on delamination initiation. Results were again evaluated using finite element analyses.

The present paper describes recent and on-going research performed at the National Aerospace Laboratory NLR, which aims at the derivation of a failure criterion for stiffener pop-off and the implementation of this failure criterion in PANOPT.
Firstly, the test configuration used in the current work and the experimental results in terms of failure loads and failure modes, is given. Then, the derivation of a failure criterion based on these results is presented. Subsequently, an evaluation of this criterion using experimental results from references 4 and 5 is given. Finally, conclusions and directions for future work are given.

EXPERIMENTAL INVESTIGATION

SPECIMEN DESCRIPTION

A simple test specimen configuration, similar to the configuration used in references 4 and 5, was used to determine the significant parameters which influence the strength of a skin-stiffener interface in a composite stiffened panel.

The specimens consisted of a stiffener flange with a 45° taper, bonded onto a skin laminate. The specimen width was equal to 50 mm. Specimen dimensions are given in figure 1, in which the fibre direction of a 0° ply (parallel to the stiffener axis) is also indicated.

The experimental programme encompassed 5 skin laminates which are combined with 4 flange laminates, as given in tables I and II. The laminates were made using Fibredux 6376C HTA prepreg, with a nominal thickness of 0.181 mm. The adhesive used to bond the flange and skin laminates was FM 300M.

First, the laminated plates for skins and flanges were manufactured and cured, except for skin laminate S5. Flanges were then cut to the required shape. Subsequently, the skins and flanges were co-bonded, except for skin S5. Skin S5 was assembled in a ‘wet' condition with the cured flange F4. Finally, all specimens were cut to the indicated dimensions.

EXPERIMENTAL PROCEDURE

The specimens were loaded in four-point bending in the same test rig as used in earlier research (Ref. 2). A schematic representation of the loading configuration is given in figure 2.

Load was applied under displacement control, with a constant loading rate of 2 mm/min for the specimens with thinner skins (skins S1 and S2) and with a constant loading rate of 1 mm/min for the specimens with the thicker skins (skins S3, S4 and S5).

During the test, the mid-span deflection was monitored using two laser displacement transducers, which were plotted against the applied load. The displacement of the cross head was also monitored. Moreover, the specimen were monitored visually during loading using a photocamera which was zoomed in on the flange region. For several tests, acoustic emission monitoring equipment was also used.

A picture of the experimental set-up is shown in figure 3.

EXPERIMENTAL RESULTS

The delamination onset moments, which were found for the various specimens, are given in table III.

It was established that the specimens, containing the same skin laminate, exhibited a similar behaviour. Some observations for each set of specimens is given in this section.

Delamination could not be induced in the specimens with skin S1 using the current test configuration. For these specimens the magnitude of the deflection was so large that slippage occurred. The moment given in table III is the maximum moment applied until the test was stopped.

The load-deflection curve for specimens containing skin S2 showed a decrease in load when a delamination was formed, and the point of delamination onset could therefore be determined easily. Non-linear behaviour was noted just before the formation of the delamination.

Also, the graph of the cumulative acoustic emission energy versus time showed a sharp increase in energy, which corresponded to the formation of a delamination.

The photographs taken during testing and post-mortem inspection of the specimens showed that delaminations were formed between the 0° and +45 layers on the right hand side of the specimen and between the +45° and -45° layers on the left hand side of the specimen. A matrix crack in the outermost 0° ply was observed at some stage before the formation of a delamination. A photograph of a specimen containing delaminations on either side is given in figure 4.

The load-deflection curve for specimens containing skin S3 had an area of non-linear behaviour which was quite large, and a drop of the applied load occurred in most instances only at final failure, making it more difficult to establish the point of delamination onset.

The acoustic emission equipment did not provide a clear-cut indication of delamination onset either: the increase in the cumulative acoustic emission energy was quite gradual throughout the loading process upto the point of final failure.

The photographs taken during testing and post-mortem inspection of the specimens showed that delaminations were formed in the adhesive layer on the right hand side of the specimen and between the +45° and 0° layers on the left hand side of the specimen. Figure 5 shows a delamination between the +45° and 0° layers on the left hand side of a specimen. Substantial growth of the delamination was seen in some instances. On the left hand side a jump of the delamination to the adjacent interface between the 0° and -45° layers was observed.

The results obtained for specimens with skin S4 were very similar to those obtained for specimens containing skin S2, albeit at considerably higher loads. The non-linearity prior to delamination was absent for these specimens.

The delamination locations were the same as found for specimens containing skin S2. The formation of a delamination in specimen S4F3 is shown in figure 6.

The results for the specimens containing skin S5 were again quite similar to those obtained for the specimens containing the skin S3. For this specimens the only viable method to determine the delamination onset load was visual inspection, since the onset of delamination was not evident on the load-deflection curve.

Delamination was observed between the +45° and -45° layers on the left hand side of the specimen.

RESULTS FROM EARLIER INVESTIGATIONS

The results obtained earlier and reported in reference 2 were again incorporated in the current work since the parameters which were used earlier readily complement the parameters used in the current work.

Specimen description

The specimens used in reference 2 consisted of a blade-type stiffener bonded onto a skin laminate. The stiffener flange was not tapered. The specimen width was equal to 50 mm. The overall dimensions of the specimens were the same as given in figure 1.

The experimental programme encompassed 4 different skin lay-ups, three different stiffener lay-ups and for each stiffener lay-up one or two variants with either a thicker stiffener blade, which was obtained by adding a centre laminate to the blade, or a wider stiffener flange. The laminates were made using Fibredux 6376/T400H prepreg, with a nominal thickness of 0.181 mm. The adhesive used to bond the stiffener to the skin was FM 300K.
The skin and stiffener identification of all specimens is given in table IV.

Experimental procedure

The same test set-up as shown in figure 2 was used to load the specimens in four-point bending. The test were performed under displacement control with a constant loading rate of 1 mm/min. Specimens were also tested under lateral tension, in which the load is applied to the skin laminate only. The tests were performed under displacement control with a constant loading rate of 1 mm/min. During the tests, the applied load and the cross head displacement were monitored. Photographs were taken during the testing.

Experimental results

All specimens loaded in four-point bending showed a similar failure behaviour. At a certain load level a crack initiated in the fillet of the bond layer. After a further load increase, a delamination formed either in the bond layer or in the first layer of the skin laminate. The bending moments at delamination initiation for all specimens are given in table V.

The failure behaviour of the specimens loaded in lateral tension (one specimen for each configuration) was quite similar to that of the specimens loaded in four-point bending. The loads at delamination initiation for all specimens are given in table VI.

EVALUATION OF EXPERIMENTAL RESULTS

OBSERVATIONS AND INTERPRETATION OF EXPERIMENTAL RESULTS

The delamination onset moments for the specimens tested in the current programme as given in table III are shown in figure 7. The delamination onset moments for the specimens

tested in four-point bending in the earlier programme as given in table V are shown in figure 8. The delamination onset loads for the specimens tested in lateral tension in the earlier programme as given in table VI are shown in figure 9.

In figure 7 it is seen that the variation in flange lay-up did not have a significant influence on the delamination onset moment. This might be expected, since the delamination location is in the skin and the interaction between flange and skin is governed by the bending stiffnesses of the flanges which are quite similar for the flange laminates in the current programme.

However, the same is observed for the delamination onset moments from the earlier research shown in figure 8. Here it is seen that for the thinner skin laminates 1a and 1b neither variation in stiffener lay-up nor variation in web thickness had a significant influence on the delamination onset moment. The absence of influence of either stiffener lay-up or web thickness is also observed for the skin laminate 2b. For skin laminate 2a it was again observed that the stiffener lay-up had no significant influence, but for this laminate an increase in web thickness (configuration 2a1c) or widening of the stiffener flange (configuration 2a3b) appeared to have a decreasing influence on the delamination onset moment.
The absence of an influence of the stiffener lay-up on the delamination onset moments is unexpected, especially in view of the variation by more than a factor 3 of the bending stiffnesses of the stiffener laminates.

In figure 9 it can be seen that neither variation in stiffener lay-up nor variation in the web thickness had a significant influence on the delamination onset load for all skin laminates.

Observations of the delamination locations revealed that delamination always occurred on either side of the 45° layer nearest to the flange. A schematic representation of the situation at delamination onset is given in figure 10, both for the configuration in which a 45° layer is situated adjacent to the flange and for the configuration in which a 0° layer is situated between the first 45° layer and the flange.
These findings are similar to the typical failure patterns described in reference 4.

CRITERION DEFINITION

Based on the above observations (no significant influence of flange lay-up, and delamination initiation occurring at the 45° layer nearest to the flange), it is postulated that the average in-plane normal strain perpendicular to the fibre direction and the average in-plane shear angle in the 45° layer nearest to the flange govern the initiation of a delamination.

Obviously, the ratio between the normal strain perpendicular to the fibre direction ε_{22} and the shear angle γ_{12} depends on the skin laminate. A laminate analysis programme LAP (Ref. 6) was used to obtain the normal strain perpendicular to the fibre direction ε_{22} and the shear angle γ_{12} as functions of the applied moment or as functions of the applied lateral force. The initial strains caused by the curing process, are also taken into account.

For the evaluation of the experimental results, the following material parameters were used for the prepreg materials Fibredux 6376C HTA and Fibredux 6376/T400H:

E_x = 137000 MPa
E_y = 9500 MPa
G_{xy} = 5100 MPa
ν_{xy} = 0.3

α_x = -1 10^{-6} K^{-1}
α_y = 3 10^{-5} K^{-1}

A temperature difference of -150 °C (from 170 °C to a room temperature of 20 °C) was used in the determination of the initial strains.
For the specimens with skin laminate S2 and S4 the presence of the matrix crack in the outermost 0° layer was taken into account by using the following material properties for the outermost 0° layer:
E_x = 137000 MPa
E_y = 1.10^{-5} MPa
G_{xy} = 1.10^{-5} MPa
ν_{xy} = 0

Thereby, this layer is not capable of carrying any load but partly restrains the Poisson's contraction of the laminate.

Evaluation of the tests on specimens with various skin laminates rendered a failure envelope in the ε_{22}-γ_{12} plane. As an example, ellipses are used to fit to the current data sets:

$$\left(\frac{\varepsilon_{22}}{\varepsilon_{22}^{f}} \right)^2 + \left(\frac{\gamma_{12}}{\gamma_{12}^{f}} \right)^2 = 1 \quad (1)$$

The failure envelope for the specimens tested in the current programme is given in figure 11. The failure strains used to compose the criterion were 0.5 for ε_{22}^{f} and 1.75 for γ_{12}^{f}. As can be seen, the variation in the ratio of ε_{22} and γ_{12} is only minor for the skin laminates S1, S2, S3 and S4. The ratio is approximately equal to 0.4. The ratio of ε_{22} and γ_{12} for skin S5 is approximately equal to 0.25.
The criterion brings together the results for specimens with the thinner S2 laminate and the results for specimens with the thicker S3, S4 and S5 laminates. The plotted strains for specimens with skin S1 pertain to the maximum loads during the tests, which were not sufficient to cause delamination. Clearly, the results obtained for skin S1 are not in line with the proposed criterion.

The failure envelope for the specimens tested in four-point bending in the earlier programme is given in figure 12. The failure strains used to compose the criterion for these experimental results were 0.35 for ε_{22}^{f} and 2 for γ_{12}^{f} which are quite similar to the values used in figure 13. It should be kept in mind that the flanges of the specimens with which these experimental results were obtained, were not tapered.
As can be seen, the ratio of ε_{22} and γ_{12} is similar for skin laminates 1a and 2a, and for 1b and 2b respectively. The sign of the shear angle, which was negative since the top layer had a -45° orientation, was changed to bring all results into the first quadrant.
For the results in figure 12 the criterion appears to be applicable: the results for specimens with thicker and thinner skin laminates, skin laminates 2a and 2b, and skin laminates 1a and 1b respectively, are equally well described; also, the results for very different laminates can be described by the proposed criterion.
It should be noted that the skin laminate 1b from the earlier programme is identical to the skin laminate S1 in the current programme. The same applies for skin laminates 2b and S3 respectively. From the fact that the criterion appears to properly describe the behaviour of specimens containing skin laminates 1b, whereas it appears to be less appropriate for specimens

containing skin laminate S1, it might be concluded that the performance of the test set-up under large deflections should be evaluated.

The failure envelope for the specimens tested in lateral tension in the earlier programme is given in figure 13. The ratios of ε_{22} and γ_{12} are slightly different under lateral tension compared to the ratios under bending, but the same observations as given above, apply. The failure strains used to compose the criterion for these experimental results were 0.3 for ε^{f}_{22} and 1.3 for γ^{f}_{12}. Again these values are quite similar to the values used in figure 12. Clearly, the mode of loading should not be an important parameter in the criterion. It is presently not clear whether the difference between the results pertaining to the lateral tension loading and the results pertaining to bending should be considered statistically significant.

CONCLUSIONS

The derived failure criteria and the failure strains as given in the previous section were used to calculate the delamination onset moments for the various skin laminates. These calculated delamination onset moments are plotted against the experimental delamination onset moments in figures 14 and 15 for the four point bending test results of the current and the earlier experimental programme, respectively. The black line in these figures indicates a perfect match between calculated and experimentally determined moments, both purple lines indicate a variation of 20 percent for the experimental results.

If a margin of ±20 percent is considered acceptable, it can be concluded that the results of the current experimental programme are described quite well, as can be seen in figure 18. The calculated moment for specimens with skin laminate S1 was found to be too conservative. The calculated moment for specimens with skin laminate S2 was almost exact. The calculated moment for specimens with skin laminate S3 was apparently slightly conservative. However, it should be kept in mind that in view of the lower than average detectability of a delamination, which may also be deduced from the large variation, the experimental results could be slightly biased. The calculated moment for specimens with skin laminate S4 was somewhat high, resulting in a non-conservative prediction. The variation in experimental results was again substantial. The calculated moment for specimens with skin laminate S5 corresponded quite well with the experimental results.

From the comparison of the calculated and the experimental results form the earlier experimental programme (Fig. 15), it can be concluded that these results are generally described quite well. The extreme values mostly pertain to specimens with a stiffener which had a thicker stiffener web or had an enlarged stiffener flange, especially as far as the specimens with a thicker skin were concerned.

EXPERIMENTAL RESULTS FROM THE LITERATURE

The applicability of the criterion was also evaluated for experimental results given in references 4 and 5.

In reference 4 results are given for a 24-ply skin with a quasi-isotropic lay-up. Specimens were similar to the specimens used in the current experimental programme. The specimen width was equal to 25 mm. Specimens were manufactured from the prepreg material IM6/3501-6. They contained either square ended (specimen code B) or tapered flanges

(specimen code T). The experimental programme encompassed three-point bending tests at a 3 inch span, three-point bending tests at a 4 inch span and four-point bending tests.

For the evaluation of the experimental results the following material parameters were used for the prepreg material IM6/3501-6:

E_x = 145000 MPa
E_y = 9600 MPa
G_{xy} = 5200 MPa
ν_{xy} = 0.3
α_x = $-3.6\ 10^{-7}\ K^{-1}$
α_y = $2.9\ 10^{-5}\ K^{-1}$
t_{layer} = 0.188 mm

A temperature difference of -150 °C (from 170 °C to a room temperature of 20 °C) was used in the determination of the initial strains.

The specimens with a square ended flange were unadvertently manufactured with a slightly different lay-up. The difference in lay-up is taken into account in the determination of the strains. The sign of the shear angle was changed to bring all results into the first quadrant. In figure 16 the calculated strains at failure ε_{22} and γ_{12} are given. The most salient observation is the considerably lower strains at failure for these specimens in comparison to the strains at failure given in figures 11 to 13: the strains are less than 50 percent of the strains given there. As can be seen, the ratio of ε_{22} and γ_{12} is quite different for the skin laminate combined with the square ended flanges and the skin laminate combined with the tapered flanges. As a result of the low mechanical strain levels, the relative influence of the curing strains is larger.

For the tapered specimens the strains at failure are similar for all three loading conditions. For the square ended specimens the strains at failure obtained using the three-point bending tests are somewhat lower than those obtained using the four-point bending test. The variation in the results for specimens with square ended flanges is considerably less than for the specimens with tapered flanges. From the results presented here it can be concluded that the influence of a transverse load on the delamination onset was absent for specimens with a tapered flange and relatively small for specimens with a square ended flange.

Since there is only one point per configuration, it is not possible to accurately construct failure envelopes. From the available results it appears likely that the applicable failure strains would be less for square ended than for tapered specimens. The fact that the flange tapering appears to influence the delamination onset moment whereas the flange lay-up appears to have no significant influence, would merit further research.

In reference 5, results are given of four-point bending tests. Five different specimen configurations were tested: four different skin laminates (A,C,D,F), and one skin laminate with two different flange lay-ups (A, B). All flanges were tapered with a 20° taper. The specimen width was 25 mm.

The delamination was reported to have occurred in the flange for all configurations but configuration D. Therefore the proposed criterion can not be considered valid, for all configurations but configuration D. For those configurations, the strains at failure, which are shown in figure 17, should be viewed as lying inside the proposed failure envelope. The strains at failure were calculated using the same material data as used for the results of reference 4.

Comparing the rest for configurations A and B, the influence of the flange laminate lay-up on the delamination onset moment is again found to be negligible, also for delamination in the flange. The failure strain in the outermost 45° layer for configuration C is much smaller, since this layer was the second layer from the flange interface while the layer adjacent to the flange

interface had an orientation perpendicular to the flange edge (a 90° layer in the coordinate frame given in figure 1).
The strains at failure were approximately 3 times higher than those based on the results of reference 4. It should be noted that the average delamination onset moment obtained by four point bending as given in reference 4 was 645 Nmm/mm, while the average delamination onset moment obtained by four point bending as given in reference 5 was 790 Nmm/mm. The relevant bending stiffnes of the 24-ply quasi-isotropic skin laminate in reference 4 was approximately 120 Nm for all skin laminates. The difference in delamination onset moments between references 4 and 5 is not in line with the experimental results presented in this paper.

CONCLUSIONS AND RECOMMENDATIONS

CONCLUSIONS

For the skin laminates considered, a variation of the flange lay-up did not have a significant influence on the delamination onset moment in four point bending tests or the delamination load in lateral tension tests.

Observations of the delamination locations revealed that delamination always occurred on either side of the 45° layer nearest to the flange.

The proposed criterion brought together the results for specimens with the thinner S2 laminate and the results for specimens with the thicker S3, S4 and S5 laminates. The results obtained for skin S1 were not in line with the proposed criterion.

The criterion appeared to be also applicable for the results of the earlier experimental programme. The results for specimens with thicker and thinner skin laminates were equally well described. Moreover, the results for very different laminates could be described by the proposed criterion.

From the difference in behaviour observed between the the skin laminate 1b and the skin laminate S1, it was concluded that the performance of the test set-up under large deflections should be evaluated.

The mode of loading should not be an important parameter in the criterion. It is unclear whether the difference between the results pertaining to the lateral tension loading and the results pertaining to bending should be considered statistically significant.

From the comparison of experimentally determined and calculated delamination onset moments, it can be concluded that the results of the current and the earlier experimental programme can be described quite well.

The fact that the flange tapering appears to influence the delamination onset moment whereas the flange lay-up appears to have no significant influence, merits further research.

If the specimen width would be an important parameter, this might restrict the relevance of the results obtained on strip specimens to the behaviour of panels.

RECOMMENDATIONS

The applicability of the proposed criterion should be further assessed by the execution of dedicated experimental programme in which a number of skin laminates resulting in a variety of strain ratios should be incorporated. The programme should also encompass a number of flanges with various stiffnesses and tapers. Moreover, the influence of the specimen width

on the delamination onset moment should be investigated. The issue of testing thin skin laminates, which would generally be loaded upto large deflections, should also be addressed.

A correlation between the results obtained with the current simple test configuration and results from panel tests needs to be established. Possibly, bending tests on panels of an intermediate size could fill the existing gap.

Finally, when the criterion is proven to be applicable, it will be implemented in the optimization code PANOPT, so the influence of the skin-stiffener interface strength on optimal panel designs can be determined.

ACKNOWLEDGEMENTS

This investigation has been carried out under a contract awarded by the Netherlands Agency for Aerospace Programmes, contract number 01310 N.

The contributions to the programme of a student from Imperial College, ms. S. Handley, and her supervisor K. Stevens, are gratefully acknowledged.

REFERENCES

1. **P. Arendsen, H.G.S.J. Thuis, J.F.M. Wiggenraad**
Optimization of composite stiffended panels with postbuckling constraints, National Aerospace Laboratory Technical Publication NLR TP 94083 U, published in the Proc. 50th Forum of the American Helicopter Society, Washington, DC,1994
2. **H.G.S.J. Thuis, J.F.M. Wiggenraad**
Investigation of the bond strength of a discrete skin-stiffener interface, National Aerospace Laboratory Technical Publication NLR TP 92183 L, 1992
3. **H.G.S.J. Thuis**
Onvestigation into the strength of bonded joints between composite stiffeneres and skins - continuation of the investigation described in NLR TP 92183 L -, National Aerospace Laboratory Contract Report NLR CR 93279 C (in Dutch), 1993
4. **P.J. Minguet, T.K. O'Brien**
"Analysis of test methods for characterizing skin/stringer debonding failures in reinforced composite panels", *Composite materials: testing and design (Twelfth volume)*, ASTM STP 1274, R.B. Deo and C.R. Saff, Eds., American Society for Testing and Materials, 1994
5. **P.J. Minguet, T.K. O'Brien**
"Analysis of composite skin/stringer bond failure using a strain energy release rate approach", *Proceedings of ICCM-10, Whistler, B.C.*, 1995
6. *Laminate Analysis Program, User Guide*, Anaglyph Ltd, London 1996

TABLE I LAMINATE LAY-UP DEFINITION FOR SKIN (S) AND STIFFENER FLANGE SIMULATION (F)

Code	Laminate lay-up
S1 F1	[45, 0, -45, 0, 45, -45, 0, -45, 0, 45]
S2 F2	[0, 45,-45, 90, 45, -45, 90, -45, 45, 0]
S3	[45, 0, -45, 0, 45, 0, -45, 0, 45, 0, 0, -45, 0, -45, 0, 45, 0, -45, 0, 45]
S4	[0, 45,-45, 0, 45, 0, -45, 90, 45, 0, 0, -45, 90, -45, 0, 45, 0, -45, 45, 0]
S5	$[45,-45, 0, 45,-45, 90, 0, 45, -45]_s$
F3	[45, -45, 45, -45, 0, -45, 45, -45, 45]
F4	[45,-45, 0, 0, 90, 0, 0, -45, 45]

TABLE II TEST MATRIX INDICATING THE NUMBER OF SPECIMENS PER CONFIGURATION

	S1	S2	S3	S4	S5
F1	3	3	3	3	
F2	3	3	3	3	
F3	3	3	3	3	
F4					3

TABLE III EXPERIMENTAL RESULTS OF CURRENT PROGRAMME

Specimen configuration	Delamination onset moment [Nmm/mm]				
				Average	Deviation
S1F1	155.8	143.7	147.5	149	5
S1F2	136.5	145.7	148.3	143.5	5.1
S1F3	147.3	147.3	152.4	149	2.4
S2F1	148.0	145.5	143.8	145.8	1.7
S2F2	148.0	151.8	156.3	152	3.4
S2F3	165.3	154.9	148.1	156.1	7.1
S3F1	673.4	588.2	515.9	592.5	64.4
S3F2	526.8	513.0	504.4	514.7	9.2
S3F3	565.7	540.0	528.4	544.7	15.6
S4F1	477.6	558.5	477.0	504.4	38.3
S4F2	478.7	452.3	534.1	488.4	34.1
S4F3	538.8	534.1	505.5	526.1	14.7
S5F4	531.6	631.8	565.9	576.4	41.6

TABLE IV LAMINATE LAY-UP DEFINITION FOR SKIN AND STIFFENER

Skin laminates			
Code	Laminate lay-up		
1a	[-45, 45, -45, 45, -45, 45, 45, -45, 45, -45]		
1b	[-45, 0, 45, 0, -45, 45, 0, -45, 0, -45]		
2a	[-45, 45, -45, 45, -45, 45, -45, 45, -45, 45]s		
2b	[45, 0, -45, 0, 45, 0, -45, 0, 45, 0, 0, -45, 0, -45, 0, 45, 0, -45, 0, 45]		
Stiffener laminates			
Code	Laminate lay-up	Core laminate lay-up	Flange width [mm]
1a	[0, 45, 0, -45, 0, 90, 0, -45, 0, 45, 0]	-	44
1b	[0, 45, 0, -45, 0, 90, 0, -45, 0, 45, 0]	$[0_5]$	44.9
1c	[0, 45, 0, -45, 0, 90, 0, -45, 0, 45, 0]	$[0,-45,0,45,0]_s$	45.81
2a	[0, 0, 45, 0, -45, 0, 90, 0, -45, 0, 45, 0, 0]	-	50
2b	[0, 0, 45, 0, -45, 0, 90, 0, -45, 0, 45, 0, 0]	$[0,-45,0,45,0]_s$	51.81
3a	[0, 45, -45, 45, 0, -45, 0, 90, 0,-45, 0, 45, -45, 45, 0]	-	44
3b	[0, 45, -45, 45, 0, -45, 0, 90, 0,-45, 0, 45, -45, 45, 0]	-	56

TABLE V FOUR-POINT BENDING TEST RESULTS OBTAINED IN EARLIER PROGRAMME (REF. 2)

Specimen configuration	Delamination onset moment [Nmm/mm]				
				Average	Deviation
1a1a	101	109	105	105	3.3
1a1b	90.9	98.9	107	98.9	6.6
1a2a	104	124	112	113.3	8.2
1a2b	100	117	851	100.7	13
1b1a	100	92	874	93.1	5.2
1b1b	92	886	886	89.7	1.6
1b2a	73.6	863	886	82.8	6.6
1b2b	93.2	100	84	92.4	6.6
2a1a	506	454	500	486.7	23.2
2a1c	374	305	385	354.7	35.4
2a3a	472	523	431	475.3	37.6
2a3b	426	282	328	345.3	60.1
2b1a	437	460	460	452.3	10.8
2b1c	500	460	-	480	-
2b3a	397	466	385	416	35.7
2b3b	460	552	426	479.3	53.2

TABLE VI LATERAL TENSION TEST RESULTS OBTAINED IN EARLIER PROGRAMME

Specimen configuration	Delamination onset load [N/mm]
1a1a	240
1a1b	240
1a2a	240
1a2b	220
1b1a	320
1b1b	340
1b2a	300
1b2b	280
2a1a	480
2a1c	460
2a3a	480
2a3b	460
2b1a	580
2b1c	560
2b3a	620
2b3b	620

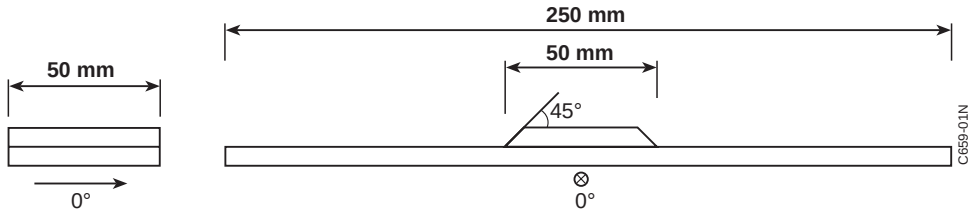

Figure 1 Specimen dimensions and reference coordinate frame for lay-up definition.

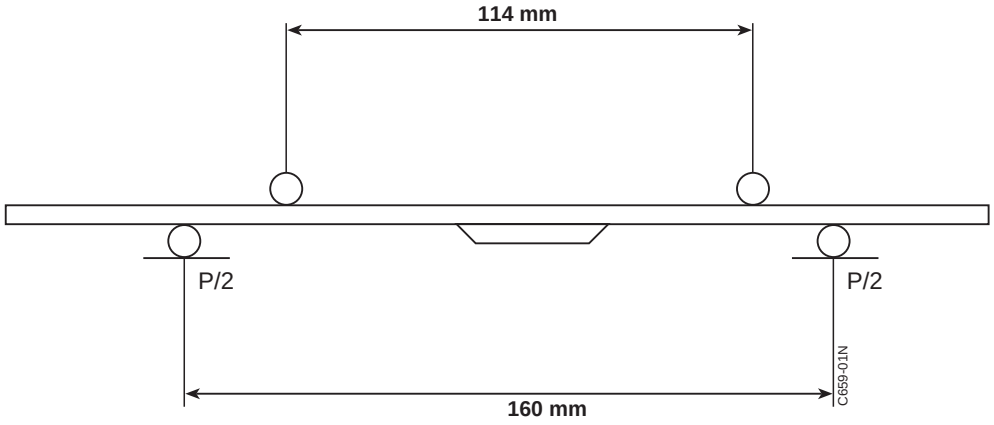

Figure 2 Schematic representation of loading configuration.

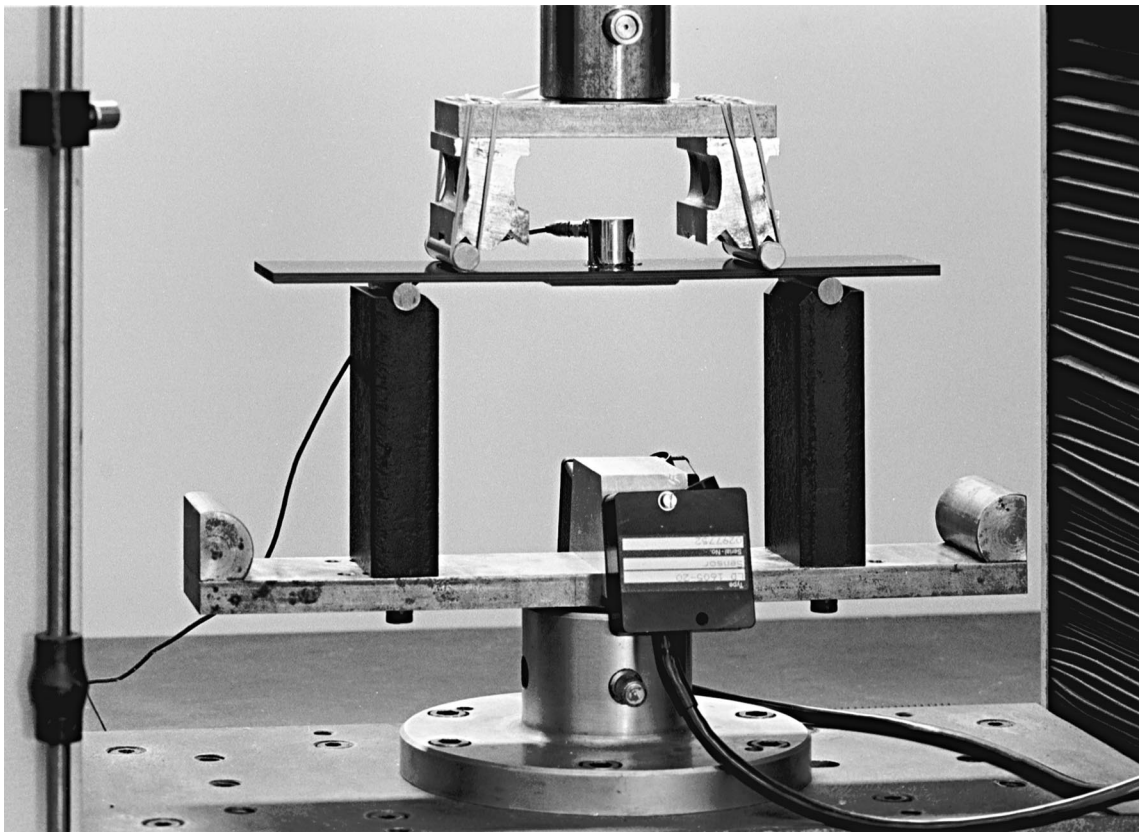

Figure 3 Experimental set-up for four point bending tests in current programme.

Figure 4 Photograph of specimen S2F1-2 containing delaminations on either side.

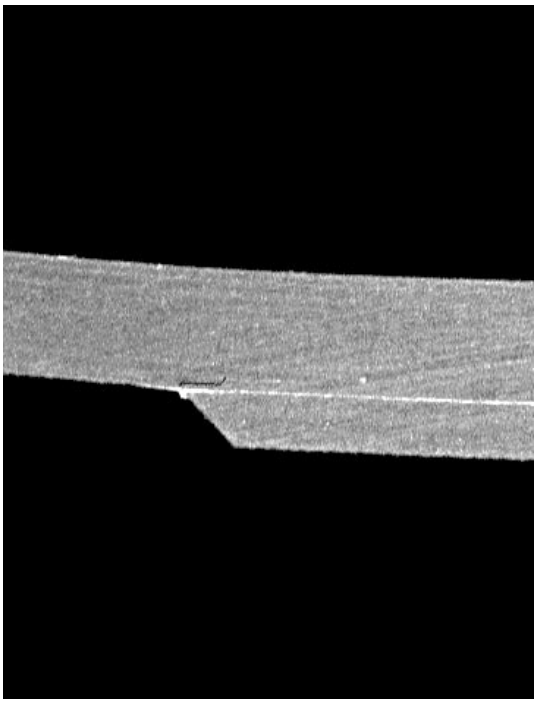

Figure 5 Initial stage of a delamination in a specimen with skin laminate S3.

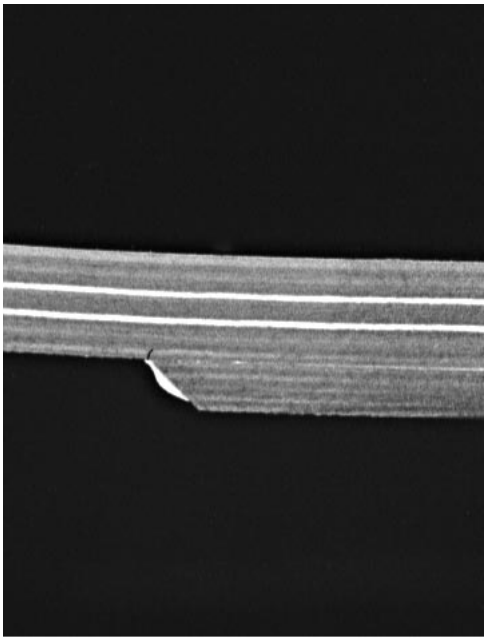

a) Cracking of the 0° layer adjacent to the flange prior to delamination

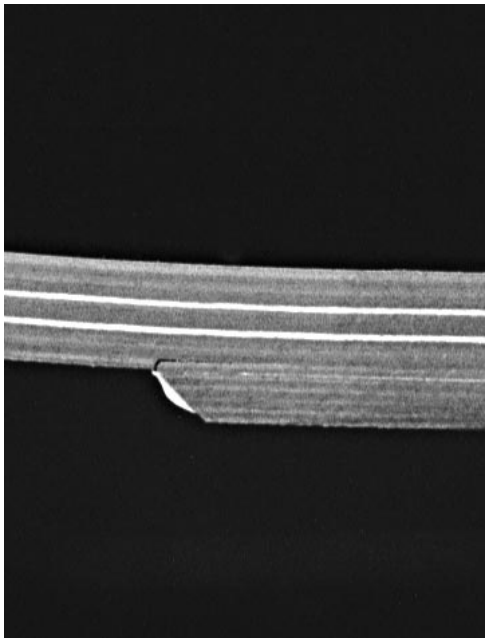

b) Formation of the delamination

Figure 6 Initial stage of a delamination in a specimen with skin laminate S4.

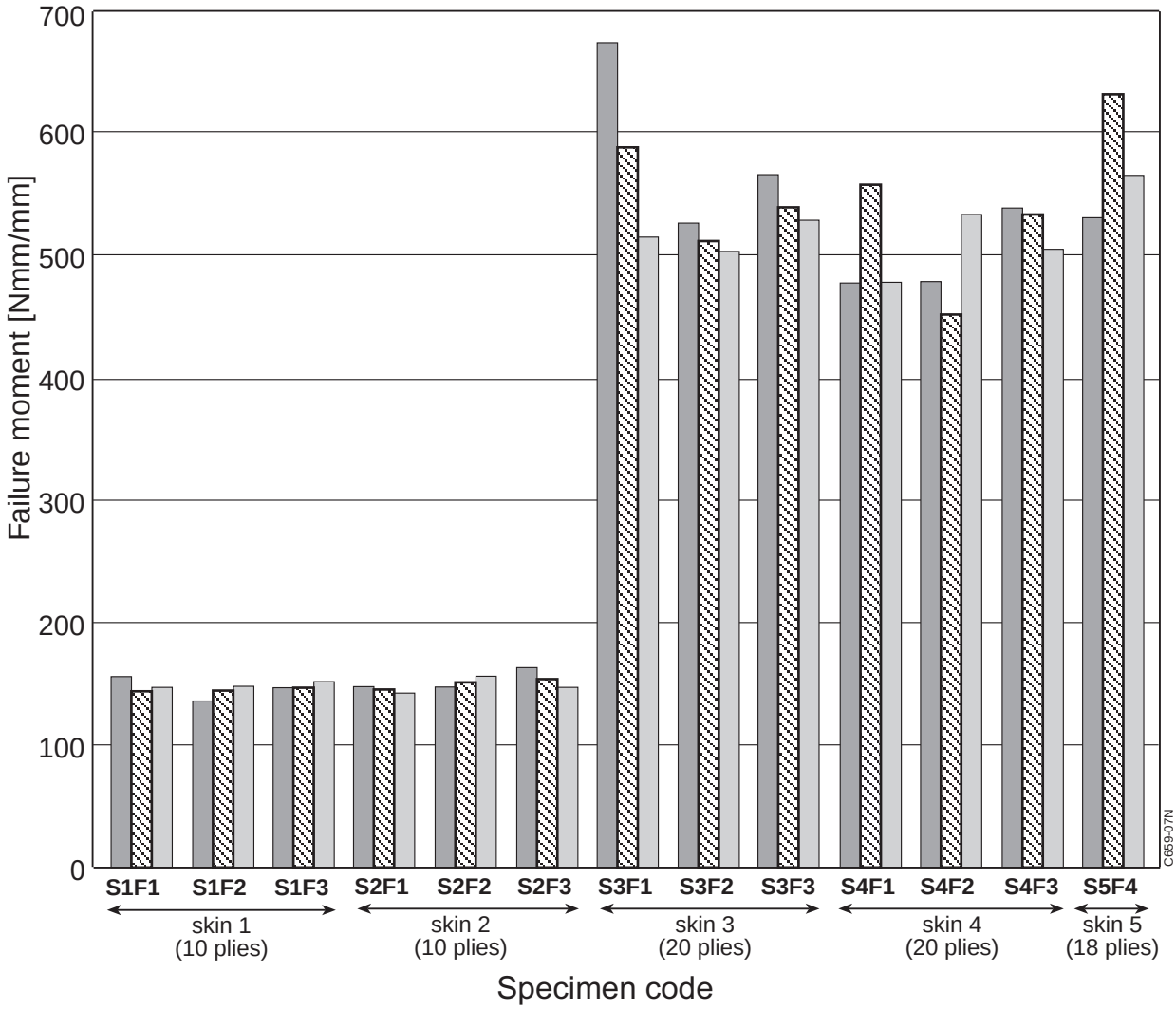

Figure 7 Delamination onset moments for the specimens in the current experimental programme as given in table III (for skin laminate S1 maximum applied moments are given which were insufficient to cause delamination).

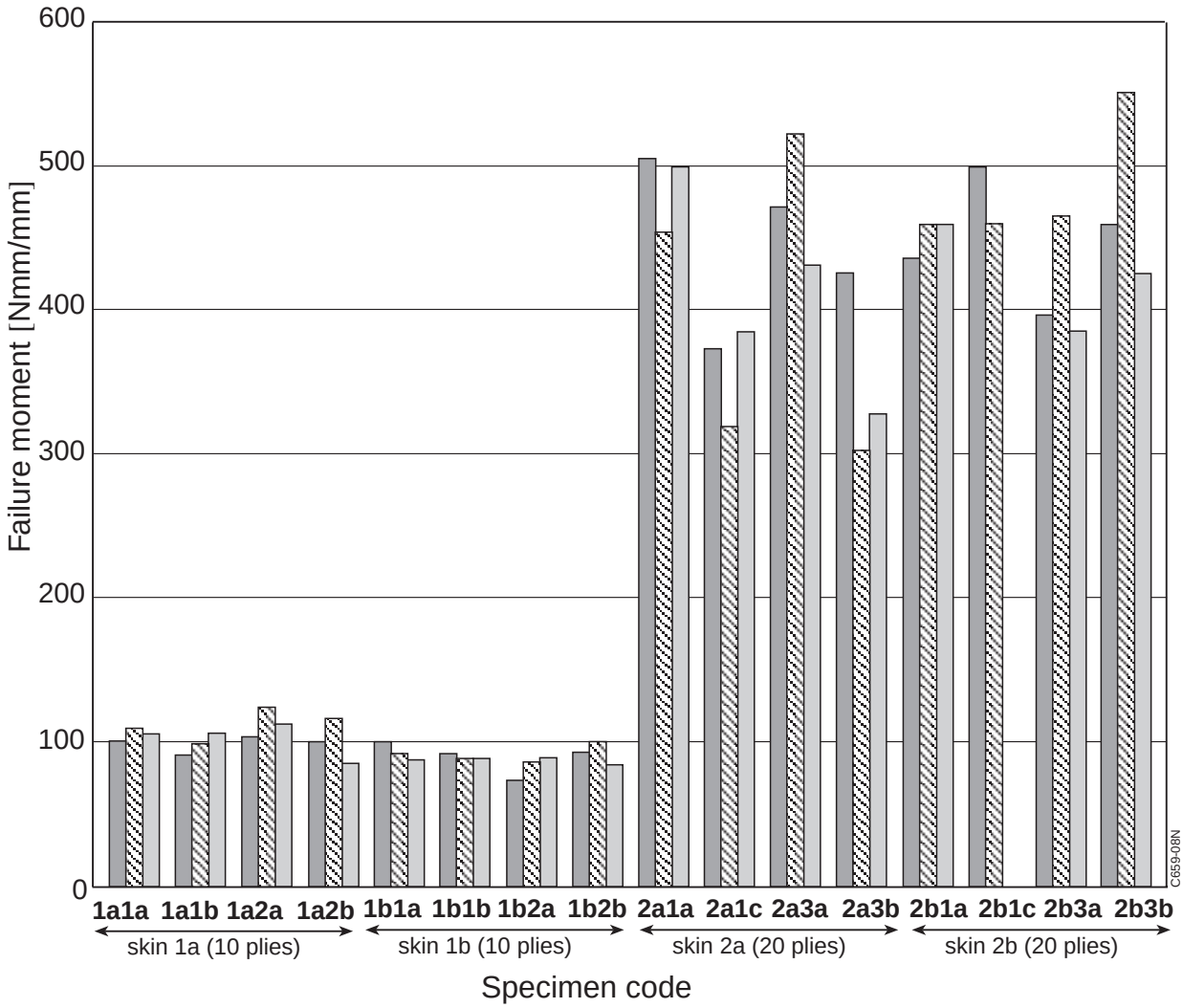

Figure 8 Delamination onset moments for the specimens tested in four-point bending in the earlier programme as given in table V.

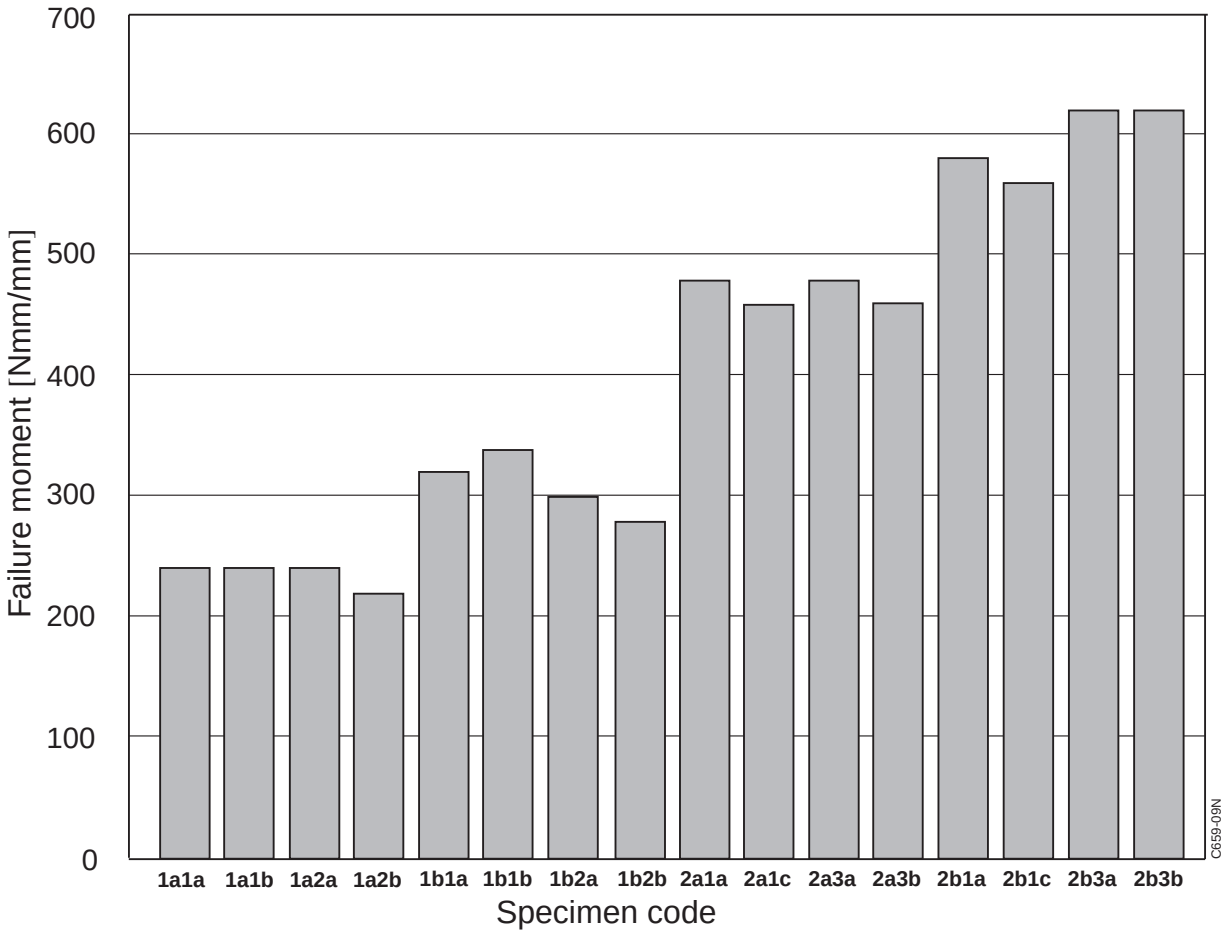

Figure 9 Delamination onset loads for the specimens tested in lateral tension in the earlier programme as given in table VI.

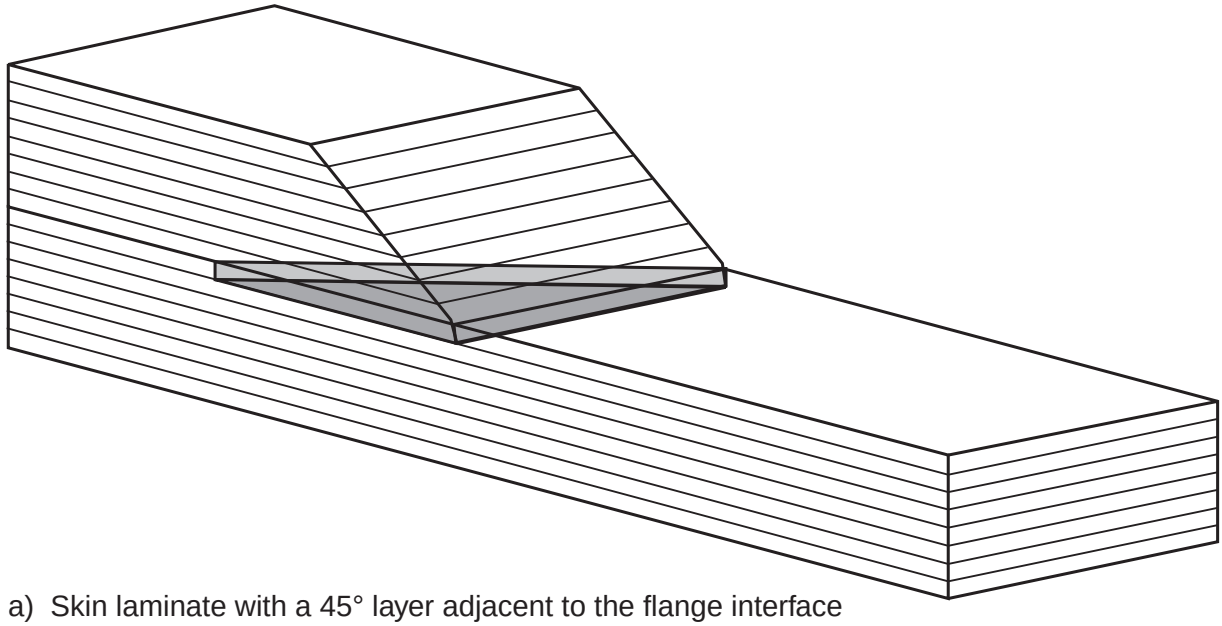

a) Skin laminate with a 45° layer adjacent to the flange interface

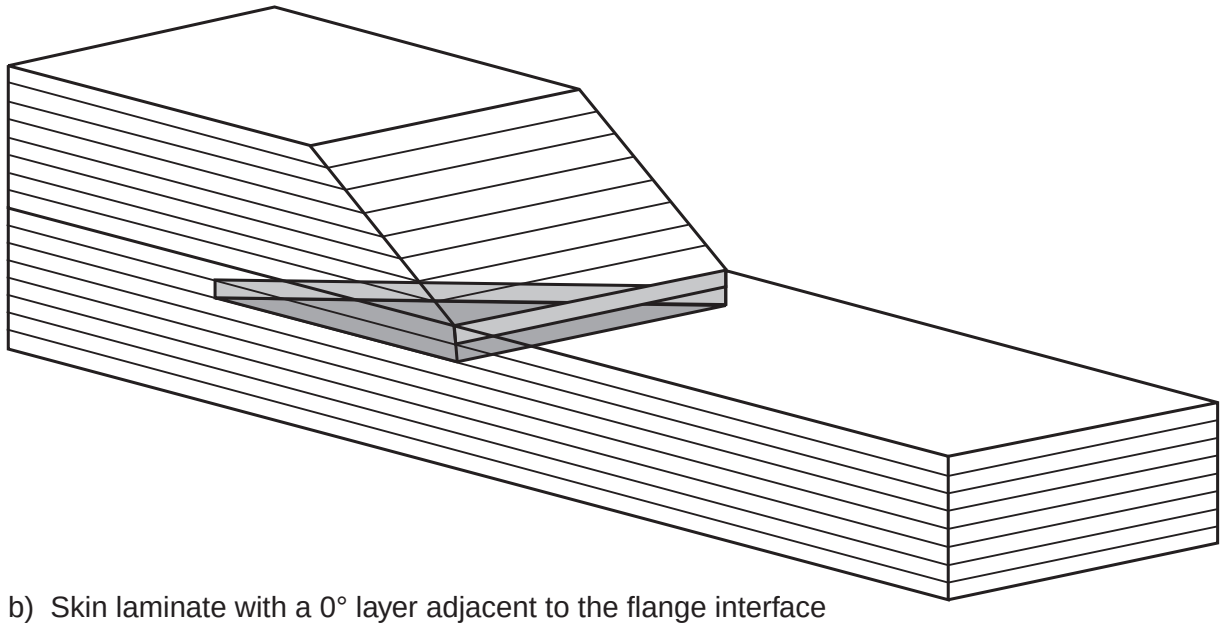

b) Skin laminate with a 0° layer adjacent to the flange interface

Figure 10 Schematic represenattion of the situation at delamination onset.

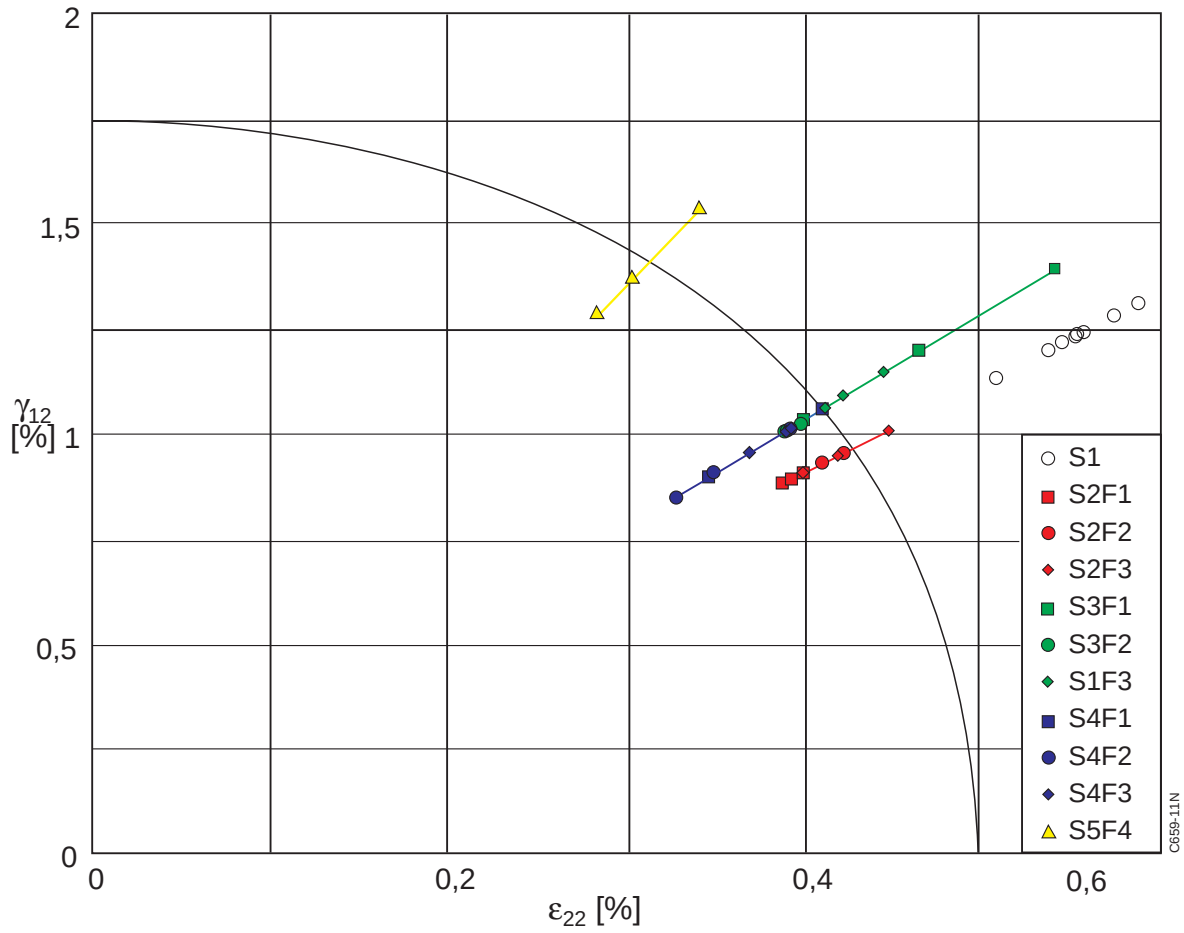

Figure 11 Failure envelope for the specimens tested in the current programme (results for skin laminate S1 pertain to the maximum applied moments which were insufficient to cause delamination).

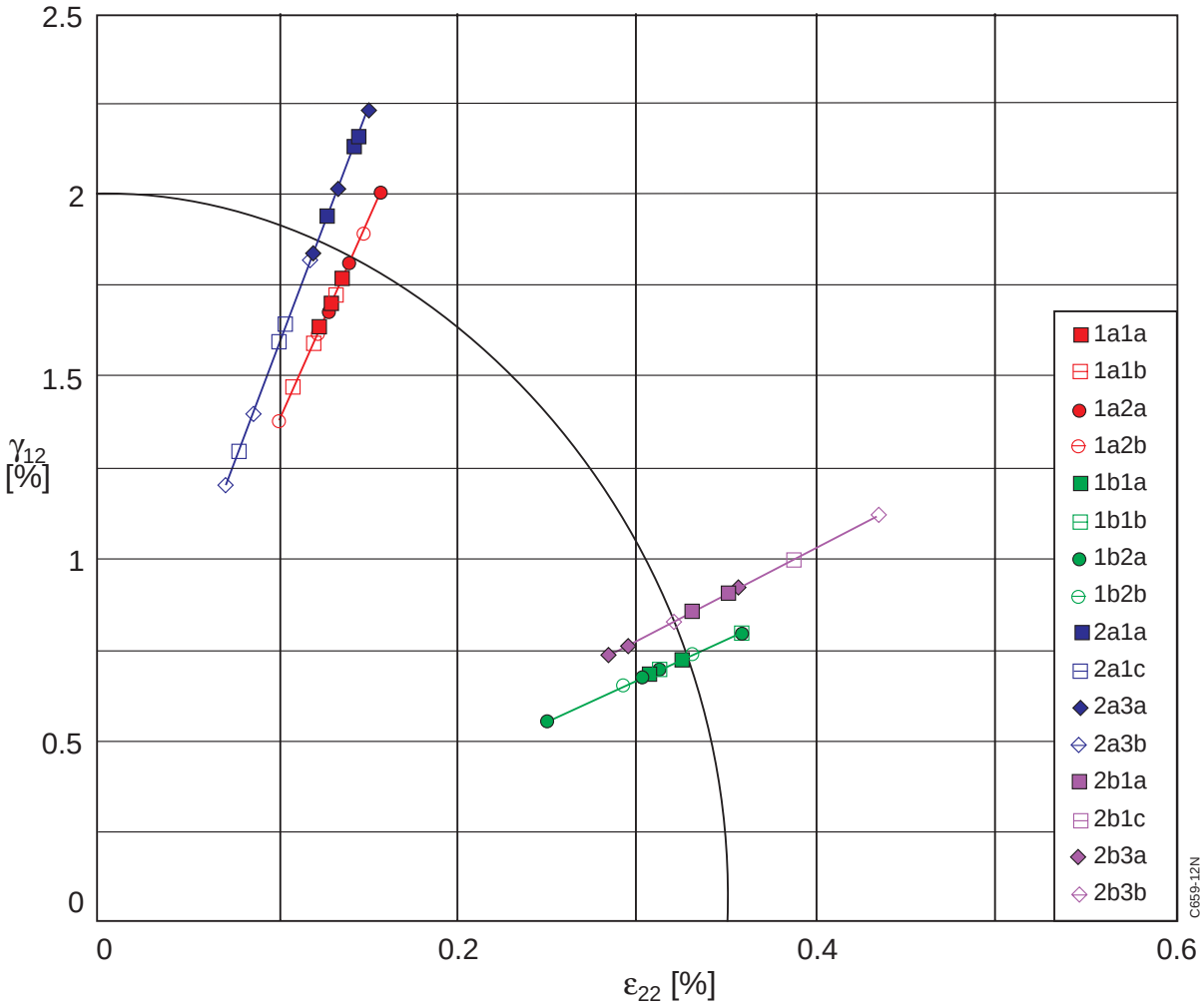

Figure 12 Failure envelope for the specimens tested in four-point bending in the earlier programme [Ref. 2].

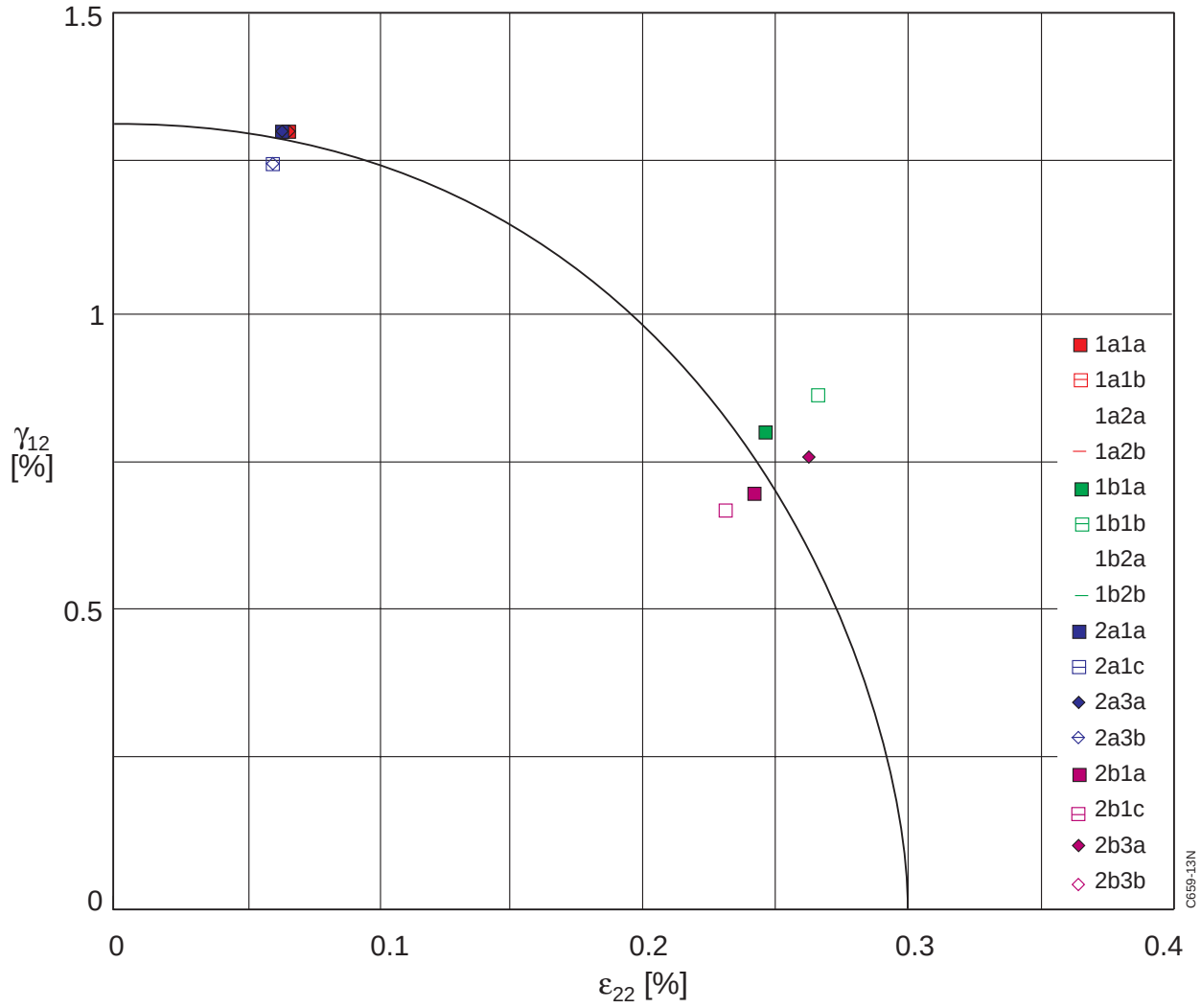

Figure 13 Failure envelope for the specimens tested in lateral tension in the earlier programme [Ref. 2].

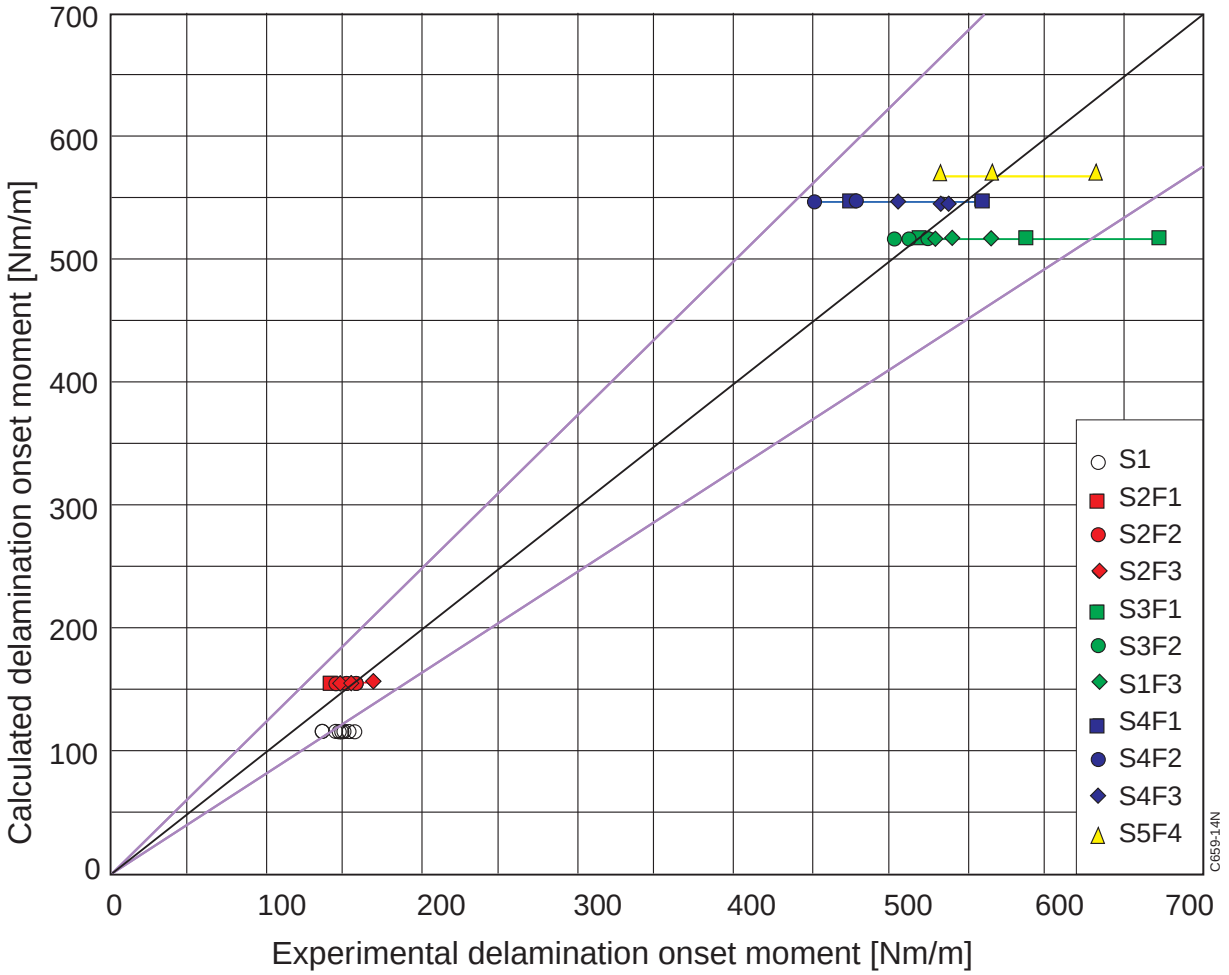

Figure 14 Comparison of the experimentally determined delamination onset moments for the specimens tested in the current programme and calculated delamination onset moments using $\varepsilon_{22}^{f} = 0.5$ and $\varepsilon_{12}^{f} = 1.75$ (experimental results for skin laminate S1 pertain to the maximum applied moments which were insufficient to cause delamination).

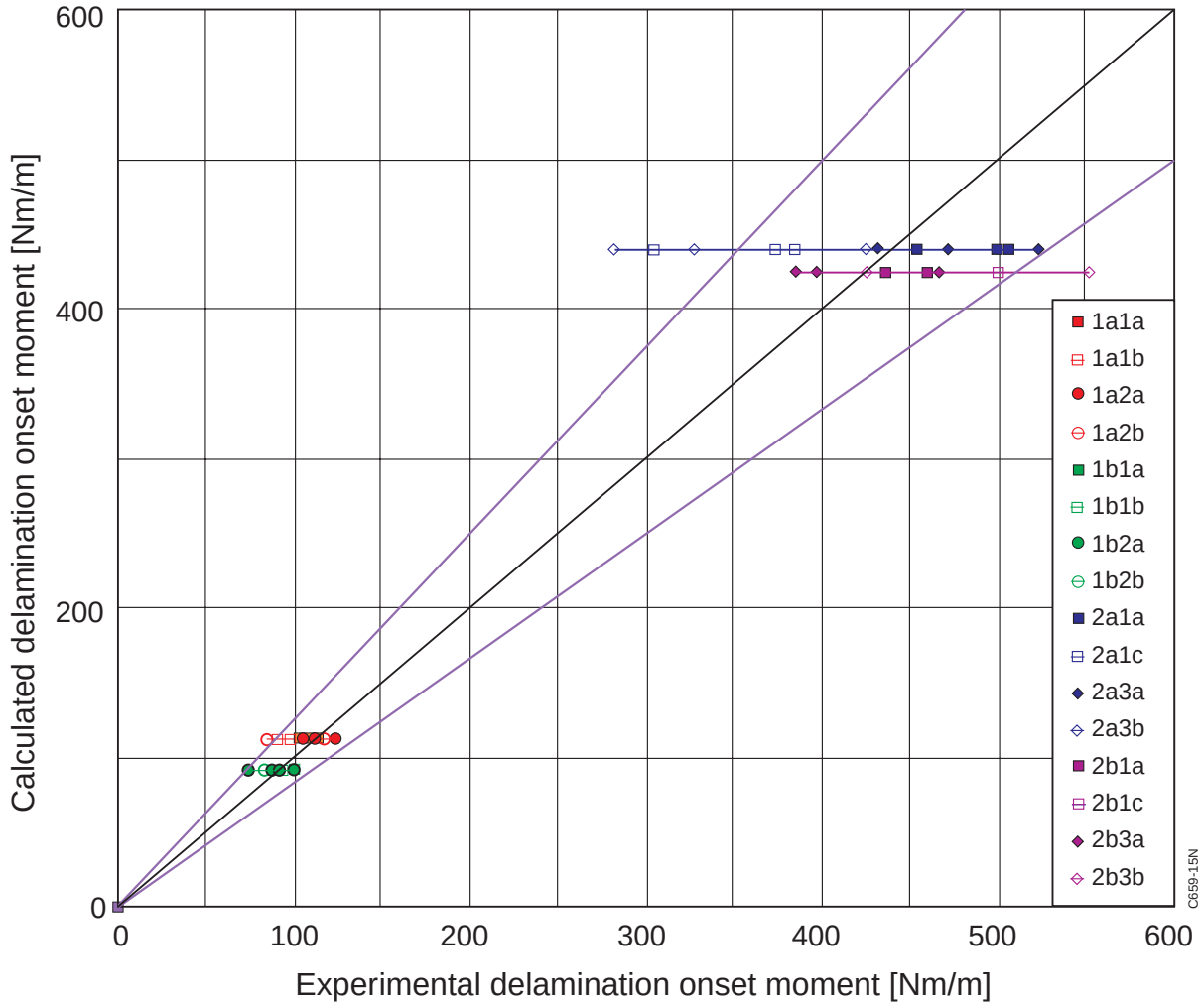

Figure 15 Comparison of the experimentally determined delamination onset moments for the specimens tested in four-point bending in the earlier programme and calculated delamination onset moments using $\varepsilon_{22}^{f} = 0.35$ *and* $\gamma_{12}^{f} = 2.0$

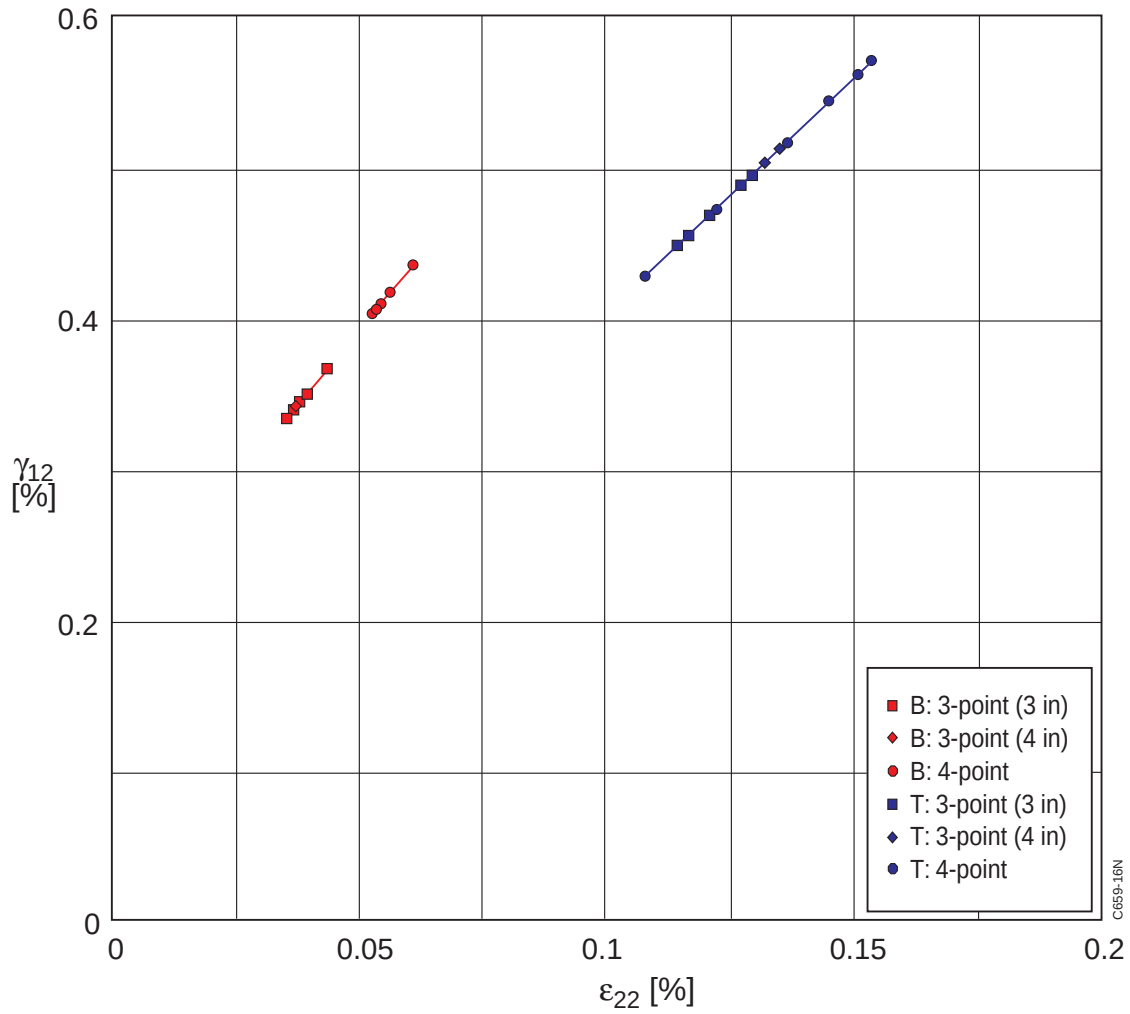

Figure 16 Calculated strains at failure for the specimens tested in three-point bending and four-point bending [Ref. 4].

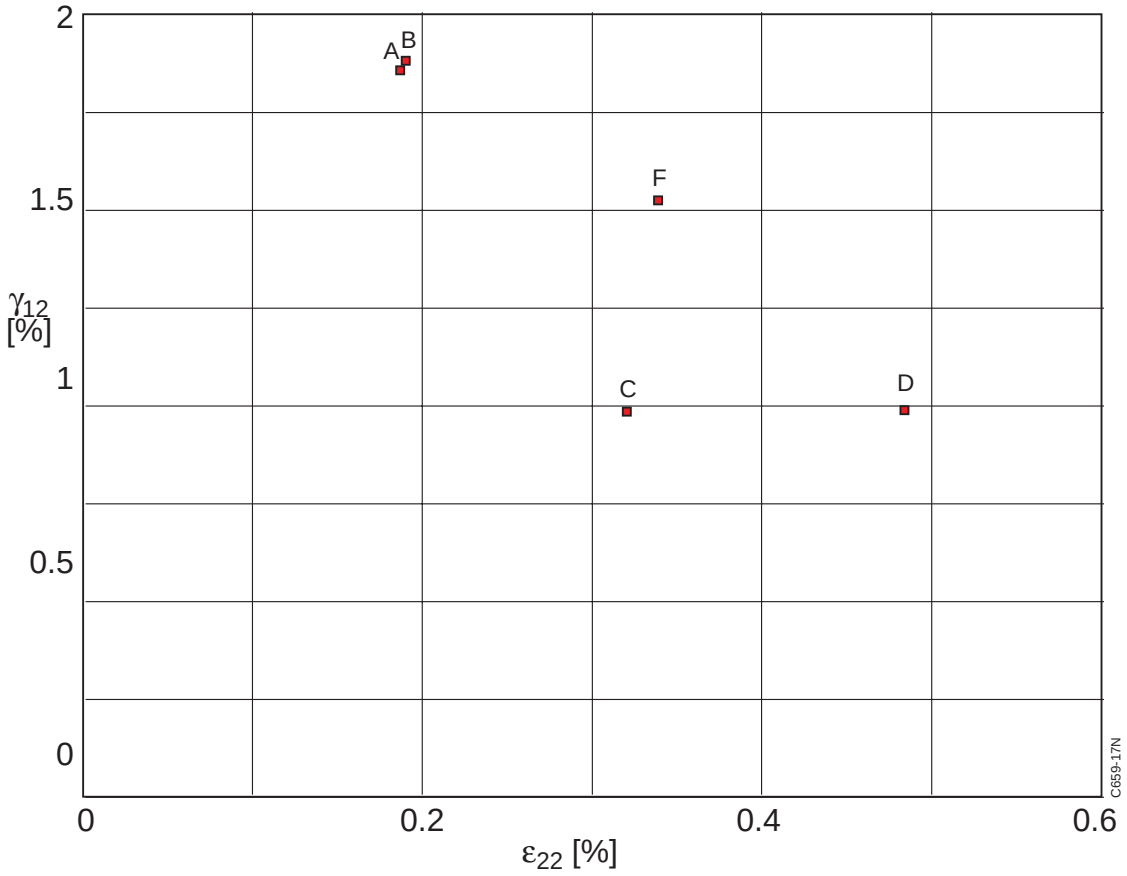

Figure 17 Calculated strains at failure for the specimens tested in four-point bending [Ref. 5].